

RESEARCH

Open Access



Determination on the thickness of superficially weathered layer of historical stones from Guanzhong area in China

Xuemei Wang^{1,2}, Hongjie Luo^{1,2*}, Haidong Yu^{3,4}, Can Xiong^{3,4}, Hui Dai^{3,4*}, Bo Rong^{1,2} and Xiao Huang^{2*}

Abstract

Superficial weathering in the form of granular disaggregation, powdering and flaking on stone surface is one of the most serious damages to stone heritages, since the surface carries most of the artistic, historical information. The determination of the thickness of the superficially weathered layer of historical stones is critical to their conservation. However, the methodology for quantitative analyses of such thickness remains very limited. In this study, we carefully study the vapor absorption and pore structure evolution of historical sandstones from Guanzhong area with respect to their weathering. We find out that the thickness of superficial weathered layer of Guanzhong sandstones can be derived by following the changes in vapor absorption or pore structure. Such data achieved from various methods developed in this work are consistent with each other and in good agreement with the results obtained by using current techniques such as drilling resistance measurement, the Ruxton method and ultrasonic testing. Among all methods used, pore size distribution analysis requires less sample preparation and measures the thickness of superficial weathered layer of Guanzhong sandstones around 7 mm.

Keywords Superficial weathering, Vapor absorption, Pore structure, Thickness of weathered layer

Introduction

China has thousands of cave temples and cliff statues, among which arenaceous based cultural heritage accounts for more than 60% [1]. However, being exposed

to natural environment for a long time, those sandstone heritages have shown severe weathering, such as superficial weathering, mechanical cracks and other forms of deterioration, greatly reducing their mechanical strength and cohesion (Fig. 1) [2–4]. Superficial weathering, in particular, has received a lot of attention in historical stone conservation. Compared with other types of weathering, it often causes greater losses of the value of the heritage, as the surface usually carries most artistic and historical information. Various forms of superficial weathering have commonly been observed, such as crust formation [5–7], granular disaggregation [8], powdering and flaking [9, 10], etc.

Research has shown that the loss of matrix and cement minerals caused by the long-term interactions between sandstone and environmental factors is one of the major reasons of superficial weathering [11, 12]. To protect the historical sandstones against such weathering, manually introducing conservation materials to the weathered

*Correspondence:

Hongjie Luo
hongjieluo@shu.edu.cn

Hui Dai
316067909@qq.com

Xiao Huang
xhuang@shu.edu.cn

¹ School of Materials Science and Engineering, Shanghai University, Shanghai 200444, China

² Institute for the Conservation of Cultural Heritage, Shanghai University, Shanghai 200444, China

³ Chongqing Key Laboratory of Paleontology and Paleoenvironment Co-evolution (Sichuan-Chongqing Joint Construction), Chongqing 400700, China

⁴ 208 Hydrogeological and Engineering Geological Team, Chongqing Bureau of Geological and Mineral Resource Exploration and Development, Chongqing 400700, China



© The Author(s) 2024. **Open Access** This article is licensed under a Creative Commons Attribution 4.0 International License, which permits use, sharing, adaptation, distribution and reproduction in any medium or format, as long as you give appropriate credit to the original author(s) and the source, provide a link to the Creative Commons licence, and indicate if changes were made. The images or other third party material in this article are included in the article's Creative Commons licence, unless indicated otherwise in a credit line to the material. If material is not included in the article's Creative Commons licence and your intended use is not permitted by statutory regulation or exceeds the permitted use, you will need to obtain permission directly from the copyright holder. To view a copy of this licence, visit <http://creativecommons.org/licenses/by/4.0/>. The Creative Commons Public Domain Dedication waiver (<http://creativecommons.org/publicdomain/zero/1.0/>) applies to the data made available in this article, unless otherwise stated in a credit line to the data.

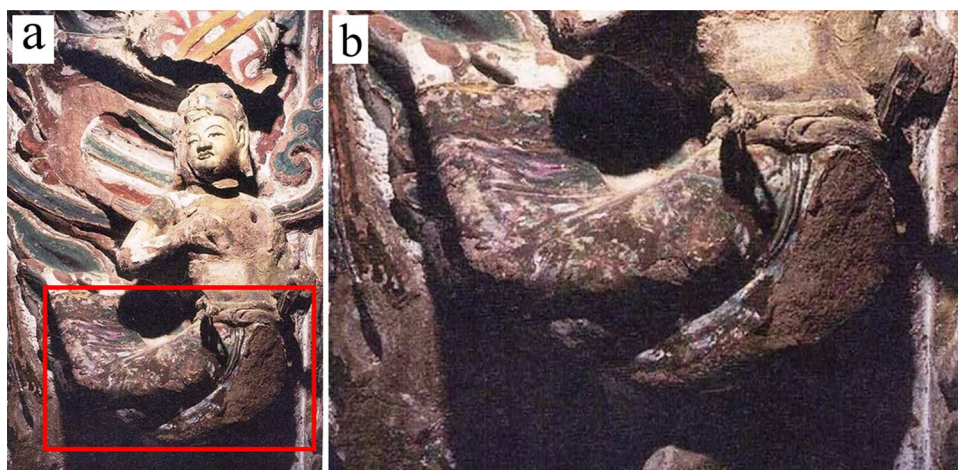


Fig. 1 Severe surface weathering of historical stone located in Guanzhong area in China. **a** Dafosi grottoes; **b** enlargement of red square area in (a)

surface is the generally adopted protocol at present. During the past decades, various conservation materials for sandstone have been explored, including inorganic materials such as high modulus K_2SiO_3 , nanolime etc. [13, 14], organic materials such as acrylic resin, silicon-based compounds etc. [15, 16], and organic–inorganic composite materials [17, 18].

However, the introduction of protective materials will change the physicochemical properties of the sandstone at certain degree. Thus, the interactions between sandstone and environmental factors, the deterioration mechanism and the key damage factors can change accordingly. Therefore, it is vital to clearly gather information such as composition, macro- and micro-structure, physical status, the leading factor causing weathering and more information of the weathered layer before taking any conservation actions. Although many protocols have been developed to investigate the mineral component [19, 20], pore size distribution [21, 22], physical and mechanical properties [23, 24] of weathered sandstones, characterizing the thickness of the superficial weathered layer has received much less attention despite its importance Additional file 1.

Quantitative analysis of the thickness of the weathered layer has been realized by multiple expensive instrumentations, such as Laser microprobe [25], nuclear magnetic resonance (NMR) [26], small angle neutron scattering [27] and X-ray computed micro-tomography (micro-CT) [28]. Drilling resistance measurement system (DRMS) is another commonly used technique to detect the thickness of weathered layer. However, DRMS results can be affected by inhomogeneity of the sandstone at the micron level, such as embedded micron-sized mineral particles [29].

It is well known that weathered and unweathered sandstones show different physical and chemical properties, such as their composition, strength, porosity, moisture absorption ability, etc. Previous research has mostly focused on characterizing those variations and trying to establish the correlation between these differences and the degree of weathering. In this paper, we carefully and systematically study the vapor adsorption and pore structure of sandstone along the direction from its surface towards its inner. The thickness of superficially weathered layer can be acquired based on analyses of these data. Both vapor adsorption and pore structure methods give out similar results which are consistent with results obtained from ultrasonic velocity test, Ruxton method [30] and DRMS. Details are discussed below.

Experimental

Description and characterization of stone samples

The sandstone used in this study is a sedimentary lithotype, from Guanzhong area in the south of Shaanxi Province, China. Stone samples were collected at the same lithological layer (Fig. 2) but 50 m north to the historical stones, which are lithologically representative and at the similar degree of weathering to the historical stones. All samples were collected as cylinders of 5 cm in diameter with various heights. The as-collected sandstones with naturally weathered surface are referred as weathered sandstone, while those whose weathered surface (4–5 cm from surface, to guarantee all weathered part is removed) are mechanically removed are referred as unweathered sandstones (Fig. 2).

The microstructure of the sandstone was analyzed using optical microscopy (OM) and scanning electron microscopy (SEM). SEM images were taken on a

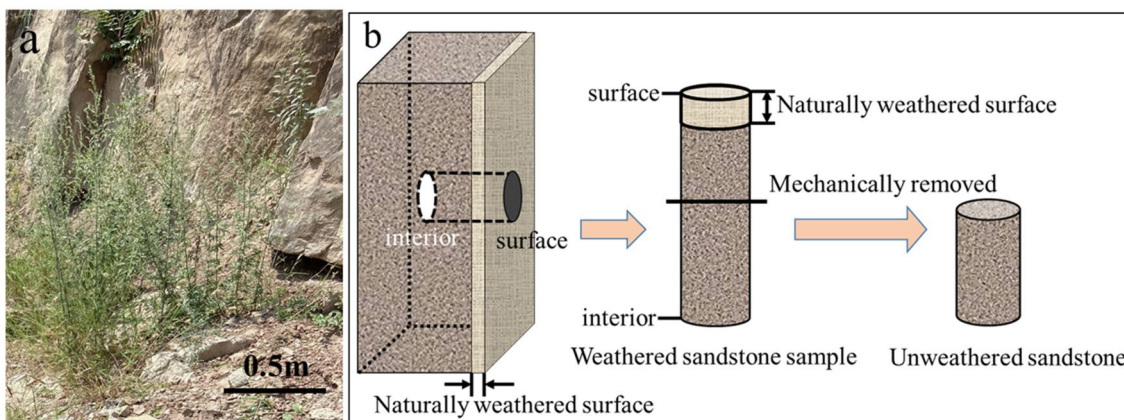


Fig. 2 a Sampling location; b Schematic diagram of sandstone sampling

Table 1 The classification standard of ultrasonic velocity ratio and weathering grade [34]

Ultrasonic Velocity ratio	Grade	Weathering extent
0–0.2	6	Residual soil
0.2–0.4	5	Fully weathered
0.4–0.6	4	Highly weathered
0.6–0.8	3	Moderately weathered
0.8–0.9	2	Weakly weathered
0.9–1	1	Unweathered

Regulus8230 (Hitachi, Japan) equipped with an EDS attachment, operating at an accelerating voltage of 2 kV~15 kV. OM images were taken on a RH-2000 microscope (Hirox, Japan). The microfibrics and mineralogical composition of the sandstones were investigated with a Leica DM2700P polarized optical

microscope on standard thin sections (30 μm in thickness). Grain type and size were recorded using Gazzi-Dickinson point counting method [31, 32]. The dry density of sandstone was acquired using an electronic densitometer (XFCNMD-3002S, Xiamen Xiongfa Instrument and Meter Co., Ltd., China) according to Chinese Standard D/ZT 0276.4–2015 [33].

The phase composition of the sandstone was characterized by X-ray diffractometer (Aeris, Panaco corporation, Netherlands) with CuKα radiation operating at 40 kV and 40 mA. A continuous scanning pattern in the scattering 2θ range of 5° to 90° with a step of 0.02° and a scanning speed of 5°/min was adopted. The chemical composition of sandstone sample was analyzed by a M4-TORNADO X-ray fluorescence spectrometer of Bruker, Germany.

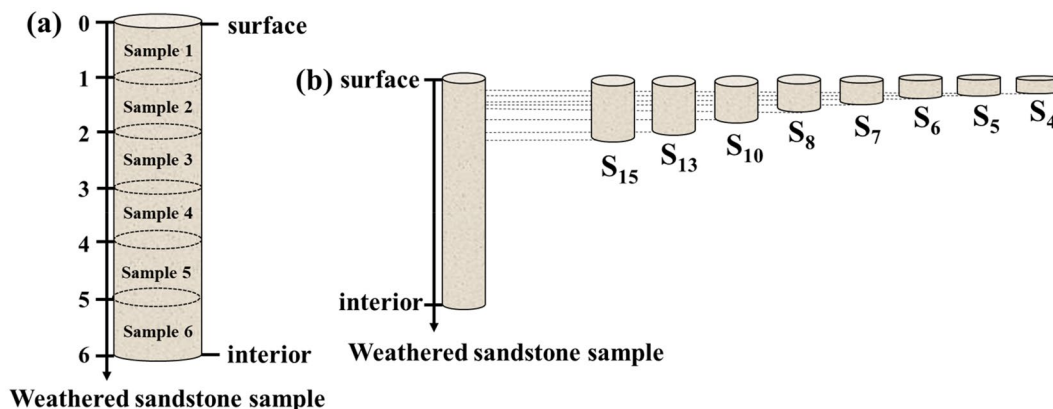


Fig. 3 Demonstration of sample preparation of (a) ultrasonic velocity method and (b) vapor absorption method. Sample S₄, S₅, S₆, S₇, S₈, S₁₀, S₁₃ and S₁₅ are columns of 5 cm in diameter and height of 4 mm, 5 mm, 6 mm, 7 mm, 8 mm, 10 mm, 13 mm and 15 mm, respectively

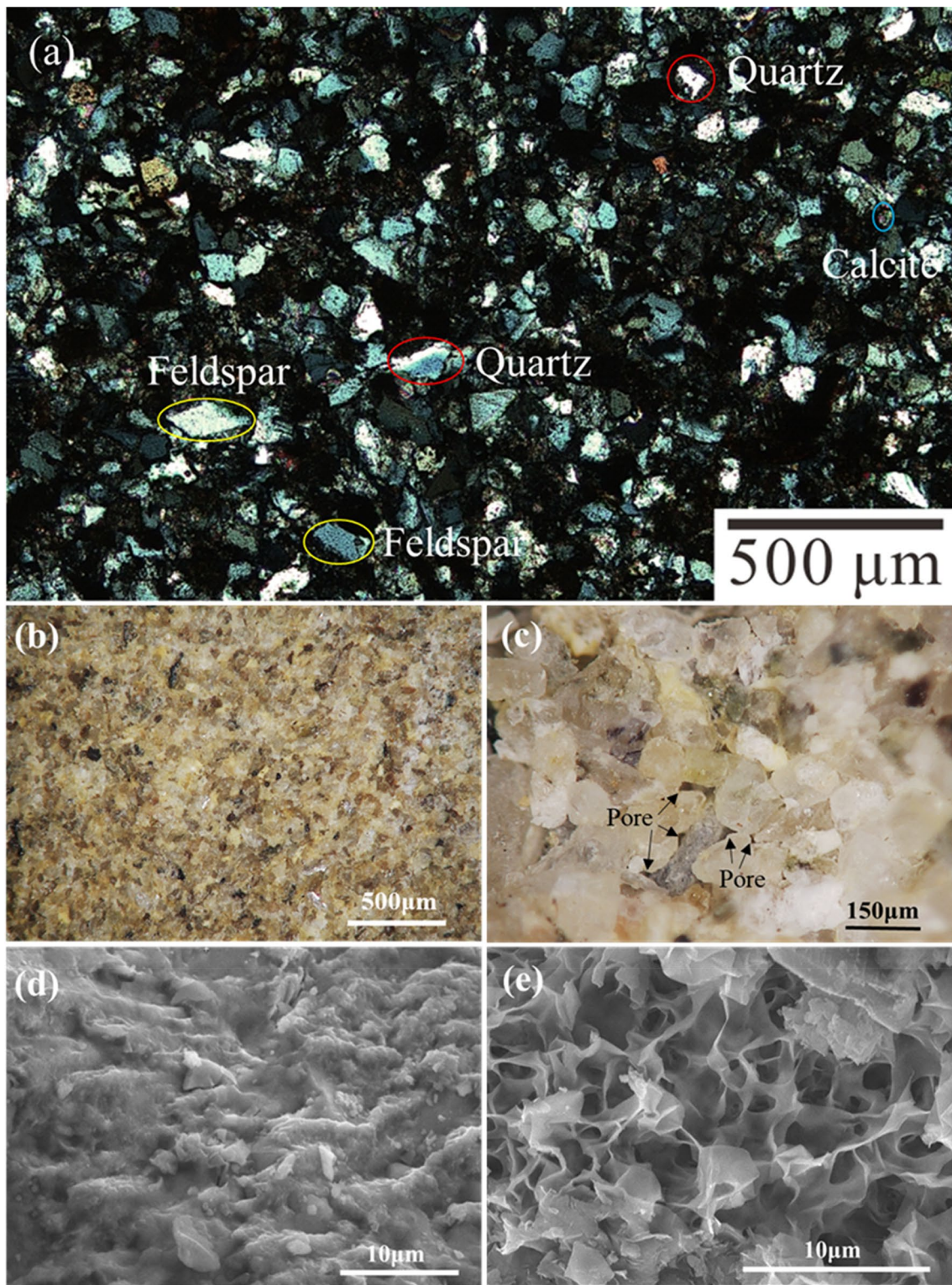


Fig. 4 a A thin-section polarized OM image of the sandstone; OM images of (b) unweathered and (c) weathered sandstones; SEM images of (d) unweathered and (e) weathered sandstones

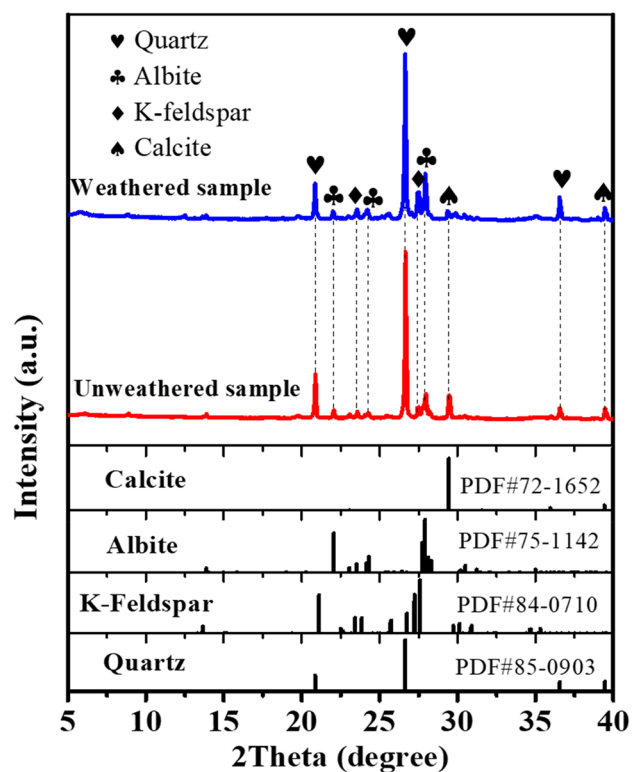


Fig. 5 X-ray diffraction patterns of the unweathered and weathered sandstones

Table 2 The chemical composition of weathered and unweathered sandstones

	Weathered (wt%)	Unweathered (wt%)
SiO ₂	63.21	65.88
Al ₂ O ₃	14.02	13.89
MgO	4.74	2.68
K ₂ O	4.23	2.61
Na ₂ O	3.86	2.39
Fe ₂ O ₃	3.54	3.94
CaO	3.29	5.27
TiO ₂	0.63	0.65
P ₂ O ₅	0.16	0.16
BaO	0.13	0.12
Total	97.81	97.59

Instrumentation and methodology for measuring the thickness of the weathered layer

The weathering degree of rock can be characterized by the ultrasonic p-wave velocity ratio K_v [34], as shown in Table 1. A sandstone was cut into six pieces (1 cm in height) as shown in Fig. 3a for the P-wave velocity test,

which was performed in accordance with the ASTM D2845-05[35], on a ZBL-U510 ultrasonic detector (Beijing Zhibolian Technology Co., Ltd., China).

Drilling resistance tests of sandstone are conducted by DRMS developed in SINT technology s.r.l. (Italy), which directly determines mechanical properties such as the hardness of stones by measuring its drilling resistance. Under the constant rotation speed (300 rpm) and drilling rate (10 mm/min), the relationship between drilling force and drilling depth is obtained. An average of 10 individual measurements was given as final result.

The chemical compositions of a sandstone at different depths (as shown in Fig. 3a) with respect to its surface were analyzed on a M4-TORNADO X-ray fluorescence spectrometer (Bruker, Germany). The molar ratio of SiO₂/Al₂O₃, referred as Ruxton ratio R, is also used to characterize the weathering degree of a sandstone [30].

Vapor absorption of sandstones was prepared as following. As shown in Fig. 3b, the as-collected sandstones cylindrical blocks (vide supra) were cut from the so-called interior direction into samples with 5 cm diameter and various heights (4, 5, 6, 7, 8, 10, 13 and 15 mm). In all samples, the weathered surface remains untouched. The sandstone samples were dried in an oven at 105 °C for 24 h [36], and then cooled to room temperature in a desiccator. The dried samples were kept in a temperature and humidity chamber controlled at 25 °C and relatively humidity (RH) of 55%. Samples were weighed daily until their weights no longer changed.

The pore structure was investigated by mercury intrusion porosimetry (MIP), using a Micromeritics Autopore IV 9500. The pore volume was measured on six samples prepared as shown in Fig. 3a. Pore size distribution analyses were performed on weathered and unweathered samples as described on Fig. 2b.

Results and discussions

Characterization of sandstones

The naturally weathered sandstone samples used in this study are mostly light brown or red. The dry densities of weathered and unweathered sandstones (see experimental for nomenclature) are 2.28 g cm⁻³ and 2.44 g cm⁻³, while the porosities of the weathered and unweathered sandstones are 19.16% and 15.67% respectively based on MIP. OM and SEM images of the unweathered and weathered sandstone sample are shown in Fig. 4. As illustrated in Fig. 4a, the sample is litho-feldspatho-quartzose sandstone with grain size distribution between 0.03 to 0.15 mm. The texture indicates that the sandstone is well-sorted and fine-grained. The major framework grains of sandstone are quartz (45–50%), feldspar (20–25%) and lithic fragments (ca. 20%). The framework grains are cemented by

approximately 5% calcite and 3% clay mineral. Trace amount of magnetite (2%) and muscovite (1%) have also been observed in the thin section (Fig. 4a). In Fig. 4, for unweathered sandstone, closely packed granular particles can be observed in both OM and SEM images, while micron-sized voids can be seen in weathered stones. Our observations of stone density decrease and porosity increase during weathering are consistent with previous reported results [37, 38].

XRD profiles of the unweathered and weathered sandstones are shown in Fig. 5. Diffraction peaks of minerals, such as K-feldspar, albite, quartz and calcite are all clearly present in the sandstone. The chemical compositions of unweathered and weathered sandstones are shown in Table 2. Both XRD and XRF results show that quartz is the major component in this type of sandstone. After weathering, the contents of K and Na increase, while that of Ca and Si decrease. Such results are consistent with slightly increase of K-feldspar, albite and decrease of calcite in XRD profiles.

Determination of the thickness of superficially weathered layer

Determination based on vapor absorption and porosity

Many physical properties of the sandstone change with the degree of weathering [37, 38]. Two common properties, vapor absorption and porosity, are carefully examined and analyzed to obtain the thickness of superficially weathered layer of naturally weathered sandstones.

Sample preparation and nomenclature for vapor absorption are described in Fig. 3b. Plot of weight gains due to vapor absorption against the distances to surface (described as sample height) is shown in Fig. 6a, which indicates weight gain increases as the sample height. Two

different linear regimes can be clearly observed with an inflection point at around 7 mm. It appears that such transition is due to significant different vapor absorption ability of weathered and unweathered sandstones. Therefore, we conclude that the thickness of superficially weathered layer of this naturally weathered sandstone is around 7 mm. The slopes in Fig. 6a further tell that the unweathered part of the stone has limited vapor absorption ability compared to weathered part.

Porosity is another property which can be used to estimate the thickness of weathered layer. A sandstone is cut into six pieces as illustrated in Fig. 3a. Porosity of each piece is measured using MIP and data are summarized in Fig. 6b. It shows the sandstone studied has weathered layer less than 1 cm.

Determination based on pore size distribution

Weathering processes not only cause progressive changes in rock porosity but also in pore size distribution, pore connectivity etc. [39] As suggested in Fig. 7a, unweathered sample mainly has smaller pores ($< 4.5 \mu\text{m}$). With weathered sample, the existing of larger pores ($> 4.5 \mu\text{m}$) is significant. The difference in pore size by MIP is consistent with microscope observations (Fig. 4). No fissures are observed in the sample used visually and by OM. Based on these observations, we hypothesize that larger pores incremented in weather stone ($> 4.5 \mu\text{m}$) are evolved from original small pores in unweathered stone due to weathering.

For superficial weathering in our case, based on data in Figs. 6, 7a, a hypothesis of pore structure evolution during weathering is proposed in Fig. 7b. We assume that the sandstone used in this work is originally structurally homogeneous (i.e., pores distribute randomly in the

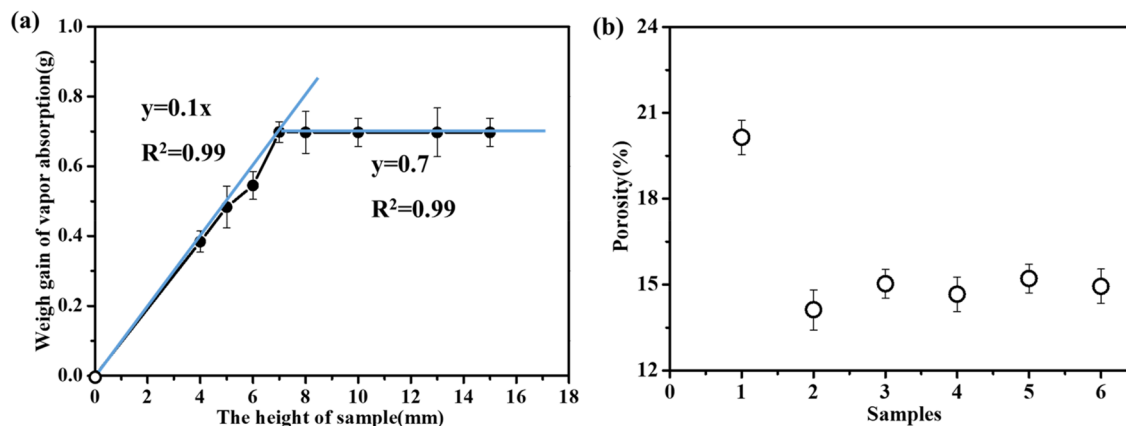


Fig. 6 **a** Plot and linear fits of stone's weight gain against height. Sample preparation and nomenclature are described in Fig. 3b. **b** Porosity of sandstone sample against sampling position. Sample preparation and nomenclature are described in Fig. 3a

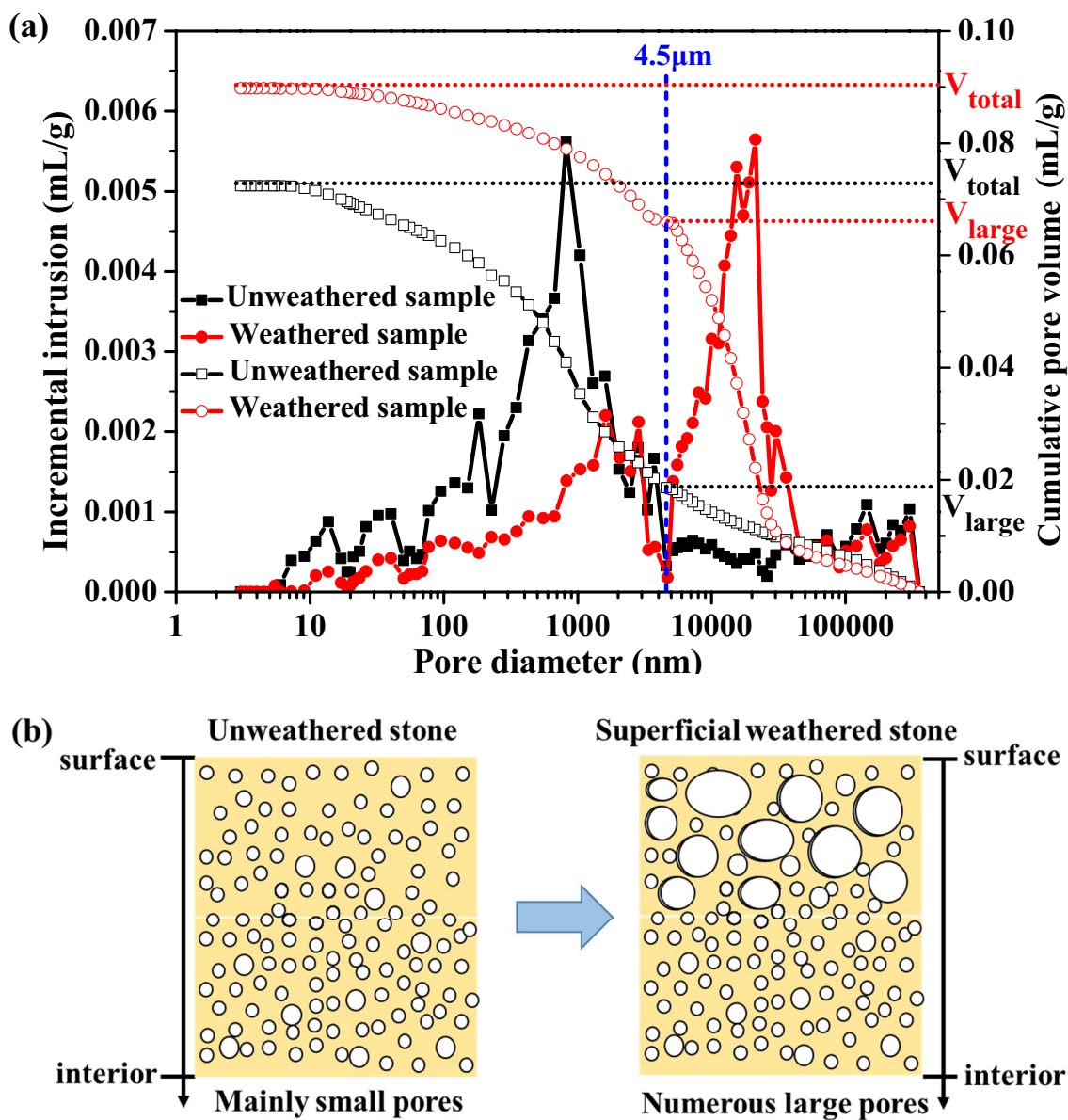


Fig. 7 **a** Pore size distribution and cumulative pore volume of weathered (red) and unweathered (black) sandstones. **b** Schematic illustration of pore structure evolution during weathering process

stone originally) and the degree of superficial weathering for this sandstone decreases from its surface to interior.

The volume percentages of small pores in the weathered and unweathered samples can be calculated based on Eq. 1 using cumulative pore volume data in Fig. 7a. In Eq. 1, $V_{small}\%$ is the small pore volume percentage, while V_{total} and V_{large} are the total and large pore volume respectively. The values are 0.26 and 0.78 for weathered and unweathered samples respectively. The

relative percentage loss of small pores can be calculated based on Eq. 2, which is 0.67.

$$V_{small}\% = \frac{V_{total} - V_{large}}{V_{total}} \tag{1}$$

$$1 - \frac{V_{small}\% \text{ in weathered sample}}{V_{small}\% \text{ in unweathered sample}} = 1 - \frac{0.26}{0.78} = 0.67 \tag{2}$$

For weathered and unweathered sandstone samples with same size (columns with 5 cm in diameter and

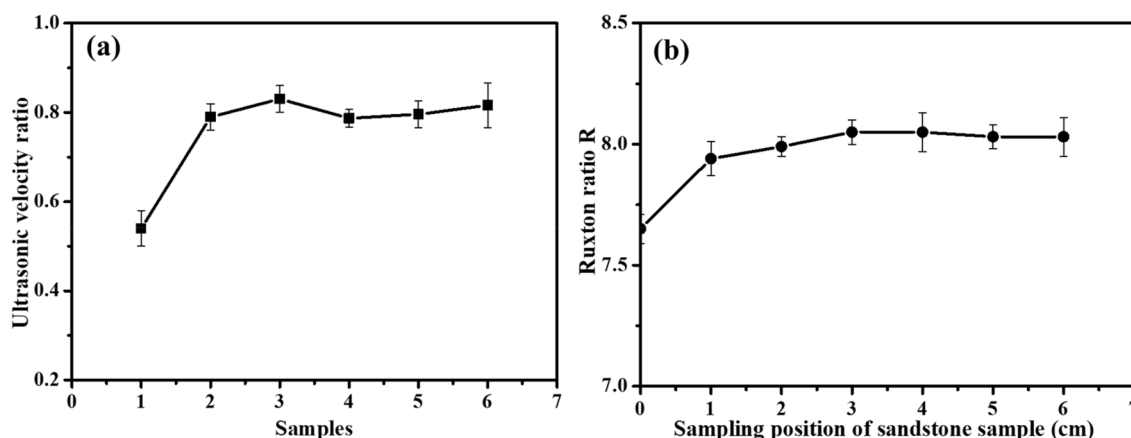


Fig. 8 a Ultrasonic velocity ratio of sandstone sample and (b) the weathering index R of chemical composition changes at different depths. $R = SiO_2/Al_2O_3$, the compositions are all in molecular proportions. Sample preparation and nomenclature are described in Fig. 3a

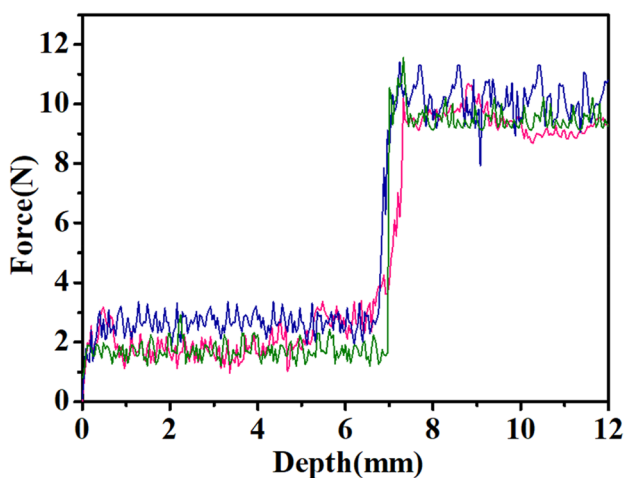


Fig. 9 DRMS results of sandstone

1 cm in height in the experiment), based on our previous assumptions, the percentage loss in small pores is linearly related to the percentage weathering in the sample. In another words, for our particular sample, 67% of the sample is weathered, while 33% remain unweathered.

Therefore, taking 10 mm as the sample height, the thickness of weathered layer of this weathered sample is 6.7 mm.

This value aligns well with previous two results. The previous two methods are relative complex, whose accuracy largely depends on how precisely the samples are prepared. Methodology on pore diameter analysis, which only requires two sample measurements, is much simpler and the accuracy mostly relies on MIP method.

Comparison with existing methodologies

In "Determination of the thickness of superficially weathered layer" section, we show three methods to characterize the thickness of the superficially weathered layer of naturally weathered sandstones. To verify the feasibility and effectiveness, results obtained from these three methods are compared with data acquired using traditional and well-accepted methods, such as ultrasonic velocity test, Ruxton method and DRMS.

For ultrasonic velocity test and Ruxton method, the sample preparation is illustrated in Fig. 3a. The data are summarized in Fig. 8. The ultrasonic velocity ratio K_v of samples 1 cm to 6 cm below the surface is larger than

Table 3 Summary of results obtained by various methods in this work

Methods	Sample preparation	Results obtained in this work
Ruxton method	Complex	Rough estimation, less than 1 cm
Ultrasonic velocity test	Complex	Rough estimation, less than 1 cm
Porosity analysis	Complex	Rough estimation, less than 1 cm
Vapor absorption	Complex	About 7 mm. Accuracy is strongly affected by the sampling procedure
Drilling resistance	Simple	About 7 mm. Heterogeneity of stone leads to the high variability of the drilling results
Pore size distribution analysis	Simple	About 6.7 mm. Accuracy is less affected by the sampling procedure

that of the surface part apparently due to superficially weathering (see Figure S1 in Supporting Info for velocity data). The ultrasonic velocity ratios of the surface part and interior of the weathered sandstone are between 0.5–0.6 and 0.8–0.9, respectively, indicating the surface part is highly weathered (see Table 1) [34]. Lower ultrasonic wave speed indicates higher porosity, which agrees well with porosity data in Fig. 6b. The changes in wave velocity ratio K_v of sandstone along the direction from the surface towards its inner show that the thickness of weathered layer in the weathered sandstone sample is less than 1 cm.

Ruxton ratio R (molar ratio of $\text{SiO}_2/\text{Al}_2\text{O}_3$) of the sandstones at different depths, which is also an indicative parameter for weathering based on composition changes [30], are also shown in Fig. 8. The R value increases firstly and then tends to be stable along the depth direction, indicating that the most severe weathering part of the sandstone is within 1 cm below the surface.

DRMS is commonly used to measure the thickness of the weathered layer in historical stones [40, 41]. The correlation curves of three samples between the drilling force and the drilling depth during the drilling process are shown in Fig. 9. Each curve is average of 10 individual measurements on same sample. All three curves show similar pattern. The sudden change of drilling force at 7 mm indicates that the thickness of weathered layer is approximately 7 mm. The comparison results among these different methods demonstrate that the thickness of superficially weathered layer of this naturally weathered sandstone obtained by vapor absorption and pore structure analyses are effective and reliable.

Conclusion

Quantitative analyses of the thickness of superficial weathered layer on weathered historical stones are important for their conservation. In this study, the vapor absorption and pore structure evolution of sandstone with respect to its weathering are carefully investigated. The thickness of superficial weathered layer can be derived by following the changes in stone's vapor absorption ability, porosity or pore size. Data acquired from these methods are consistent with each other and in well agreement with data acquired from ultrasonic velocity test, Ruxton method and DRMS.

Results obtained from different methods in this work are summarized in Table 3. Among all these methods, method based on pore size analyses seems to be simplest. Only two measurements, one on unweathered and the other on weathered stones, are required. Pore size analysis method can give out relative accurate results and the results are less affected by the sampling procedure.

Supplementary Information

The online version contains supplementary material available at <https://doi.org/10.1186/s40494-024-01206-4>.

Additional file 1: Figure S1. Ultrasonic velocity test results of rock specimens.

Acknowledgements

The authors would like to thank Dr. Gesa Schwantes and Dr. Yue Zhang from Institute for the Conservation of Cultural Heritage, Shanghai University for instructive discussions. Dr. Gesa Schwantes's help in language editing is highly appreciated. The authors are also grateful to the financial supports from the National Key R&D Program of China (No. 2019YFC1520500), Chongqing Municipal Science and Technology Bureau (No. cstc2021jcyj-msxmX1160) and Chongqing Municipal Bureau of Planning and Natural Resources.

Author contributions

XW was involved in carrying out experiments, writing original draft. HL was involved in conceptualization and review. HY, CX and HD contributed to field applications. BR provides images in Figs. 1, 4a and discussions on Fig. 4a. XH was involved in conceptualization, writing, review, editing and finalizing the manuscript.

Funding

This work is funded by National Key R&D Program of China (No. 2019YFC1520500) and Chongqing Municipal Science and Technology Bureau (No. cstc2021jcyj-msxmX1160).

Availability of data and materials

Not applicable.

Declarations

Ethics approval and consent to participate

Not applicable.

Competing interests

The authors declare no competing interests.

Received: 24 October 2023 Accepted: 9 March 2024

Published online: 18 March 2024

References

1. Data are available on the official website of the National Cultural Heritage Administration of China: http://www.ncha.gov.cn/art/2021/12/24/art_722_172472.html.
2. Feher K, Torok A. Detecting short-term weathering of stone monuments by 3D laser scanning: lithology, wall orientation, material loss. *J Cult Herit.* 2022;58:245–55.
3. Basu A, Celestino TB, Bortolucci AA. Evaluation of rock mechanical behaviors under uniaxial compression with reference to assessed weathering grades. *Rock Mech Rock Eng.* 2009;42(1):73–93.
4. Xu FG, Tang J, Gao SX. Characterization and origin of weathering crusts on Kylin carved-stone, Kylin countryside, Nanjing—a case study. *J Cult Herit.* 2010;11(2):228–32.
5. Slavik M, Bruthans J, Filippi M, Schweigstillová J, Falteisek L, Řihošek J. Biologically-initiated rock crust on sandstone: mechanical and hydraulic properties and resistance to erosion. *Geomorphology.* 2017;278:298–313.
6. Cnudde V, Silversmit G, Boone M, Dewanckele J, De Samber B, Schoonjans T, Van Loo D, De Witte Y, Elburg M, Vincze L, Van Hoorebeke L, Jacobs P. Multi-disciplinary characterisation of a sandstone surface crust. *Sci Total Environ.* 2009;407(20):5417–27.
7. Zhang H, Shi MF, Shen W, Li ZG, Zhang BJ, Liu RZ, Zhang RP. Damage or protection? The role of smoked crust on sandstones from Yungang Grottoes. *J Archaeol Sci.* 2013;40(2):935–42.

8. Gómez-Heras M, Smith BJ, Fort R. Surface temperature differences between minerals in crystalline rocks: Implications for granular disaggregation of granites through thermal fatigue. *Geomorphology*. 2006;78(3–4):236–49.
9. Michette M, Viles H, Vlachou C, Angus I. Do environmental conditions determine whether salt driven decay leads to powdering or flaking in historic Reigate stone masonry at the tower of London? *Eng Geol*. 2022;303: 106641.
10. Wang YC, Shao MS, Zhang JK, Li L, Liang XZ, Wang N. Quantitative evaluation of alteration and exfoliation in Jurassic sandstone, Chongqing Danzishi rock carvings. *China Eng Geol*. 2021;292: 106277.
11. Potysz A, Bartz W. Bioweathering of minerals and dissolution assessment by experimental simulations—Implications for sandstone rocks: a review. *Constr Build Mater*. 2022;316: 125862.
12. Mustoe GE. The origin of honeycomb weathering. *Geol Soc Am Bull*. 1982;93(2):108.
13. Nishiura T, Li ZX. Experimental study on the consolidation of fragile porous stone with potassium silicate for the conservation of cave temples in China. *Stud Conserv*. 1988;33(1):108–12.
14. Baglioni P, Giorgi R. Soft and hard nanomaterials for restoration and conservation of cultural heritage. *Soft Matter*. 2006;2(4):293–303.
15. Vicini S, Margutti S, Moggi G, Pedemonte E. In situ copolymerization of ethylmethacrylate and methylacrylate for the restoration of stone artefacts. *J Cult Herit*. 2001;2:143–7.
16. Wheeler G. Alkoxysilanes and the consolidation of stone. *J Am Inst Conserv*. 2005;46:189–91.
17. Bergamonti L, Bondioli F, Alfieri I, Alinovi S, Lorenzi A, Predieri G, Lottici PP. Weathering resistance of PMMA/SiO₂/ZrO₂ hybrid coatings for sandstone conservation. *Polymer Degradat Stability*. 2018: 147; 274–283.
18. Li D, Xu FG, Liu ZH, Zhu JQ, Zhang QJ, Shao L. The effect of adding PDMS-OH and silica nanoparticles on sol-gel properties and effectiveness in stone protection. *Appl Surf Sci*. 2013;266:368–74.
19. Liu YZ, Cai YT, Huang SB, Guo YL, Liu GF. Effect of water saturation on uniaxial compressive strength and damage degree of clay-bearing sandstone under freeze-thaw. *Bull Eng Geol Env*. 2020;79(4):2021–36.
20. Zhang LX, Zhang JK, Guo QL, Wang YW, Huang L. Quantitative assessment of weathering of cretaceous sandstone relics in Longdong area from the surface to the interior. *Sed Geol*. 2022;441: 106265.
21. Pan Z, Zhou KP, Gao RG, Jiang Z, Yang C, Gao F. Research on the pore evolution of sandstone in cold regions under freeze-thaw weathering cycles based on NMR. *Geofluids*. 2020;2020:8849444.
22. Labus M, Bochen J. Sandstone degradation: an experimental study of accelerated weathering. *Environ Earth Sci*. 2012;67(7):2027–42.
23. Chen YL, Ni J, Jiang LH, Liu ML, Wang P, Azzam R. Experimental study on mechanical properties of granite after freeze-thaw cycling. *Environ Earth Sci*. 2014;71(8):3349–54.
24. Takarli M, Prince W, Siddique R. Damage in granite under heating/cooling cycles and water freeze-thaw condition. *Int J Rock Mech Min Sci*. 2008;45(7):1164–75.
25. Aberg G, Lofvendahl R, Stijfhoorn D, Raheim A. Provenance and weathering depth of carbonaceous Gotland sandstone by use of carbon and oxygen isotopes. *Atmos Environ*. 1995;29(7):781–9.
26. Pauli J, Scheying G, Mügge C, Zschunke A, Lorenz P. Determination of the pore widths of highly porous materials with NMR microscopy. *Fresenius J Anal Chem*. 1997;357(5):508–13.
27. Coppola R, Lapp A, Magnani M, Valli M. Non-destructive investigation of microporosity in marbles by means of small angle neutron scattering. *Constr Build Mater*. 2002;16(4):223–7.
28. Crudde, V., Jacobs, P. Preliminary results of X-ray micro-tomography applied in conservation and restoration of natural building stones. X-ray CT for geomaterials, soils, concrete, rocks. 2004, 363–371.
29. Nogueira R, Ferreira Pinto AP, Gomes A. Assessing mechanical behavior and heterogeneity of low-strength mortars by the drilling resistance method. *Constr Build Mater*. 2014;68:757–68.
30. Ruxton BP. Measures of the degree of chemical weathering of rocks. *J Geol*. 1968;76(5):518–27.
31. Gazzi PL. arenarie del flysch sopracretaceo dell'Appennino modenese; correlazioni con il flysch di Monghidoro. *Mineral Petrogr Acta*. 1966;12:69–97.
32. Dickinso WR. Interpreting detrital modes of graywacke and arkose. *J Sediment Petrol*. 1970;40(2):695.
33. Chinese Standard D/ZT 0276.4–2015. Regulation for testing the physical and mechanical properties of rock-Part 4: Test for determining the density of rock.
34. Chen X, Qi XB, Xu ZY. Determination of weathered degree and mechanical properties of stone relics with ultrasonic CT: a case study of an ancient stone bridge in China. *J Cult Herit*. 2020;42:131–8.
35. ASTM D2845–05. Standard test methods for laboratory determination of pulse velocities and ultrasonic elastic constants of rock, ASTM International, West Conshohocken, PA, 2006.
36. State railway administration, state railway administration code for rock test of railway engineering (TB 10115–2014) China Railway Publishing House, Beijing (2014)
37. Wedekind W, Ruedrich J, Siegesmund S. Natural building stones of Mexico—Tenochtitlán: their use, weathering and rock properties at the templo mayor, palace heras soto and the metropolitan cathedral. *Environ Earth Sci*. 2011;63:1787–98.
38. Moses C, Robinson D, Barlow J. Methods for measuring rock surface weathering and erosion: a critical review. *Earth Sci Rev*. 2014;135:141–61.
39. Tugrul A. The effect of weathering on pore geometry and compressive strength of selected rock types from Turkey. *Eng Geol*. 2004;75(3–4):215–27.
40. Rodrigues JD, Pinto AF, Costa DR. Tracing of decay profiles and evaluation of stone treatments by means of microdrilling techniques. *J Cult Herit*. 2002;3(2):117–25.
41. Fonseca BS, Pinto AP, Rodrigues A, Pierra S, Montemor MF. On the estimation of marbles weathering by thermal action using drilling resistance. *J Build Eng*. 2021;42: 102494.

Publisher's Note

Springer Nature remains neutral with regard to jurisdictional claims in published maps and institutional affiliations.